

# Orbital-spin ordering in the striped antiferromagnetic state of iron-based superconductors

Guo-Qiang Liu

Max-Planck-Institut für Festkörperforschung, D-70569 Stuttgart, Germany

(Dated: October 24, 2018)

The magnetic properties of iron-arsenides are investigated using the LSDA+ $U$  approach. In addition to one high moment state, we find that a positive  $U$  also produces two low moment states with  $m \sim 0.4 \mu_B$  and  $m \sim 1.0 \mu_B$ . The electronic structures indicate that the low moment states originate in the strong orbital hybridization between antiferromagnetic Fe neighbors. Therefore, the geometry of the  $\text{FeAs}_4$  tetrahedron is crucial to the low moment states, which is the key to understand the negative pressure coefficient of  $T_C$  in  $\text{LiFeAs}$ . Finally, our theory suggests that the superconducting phase is an orbital-spin ordered state, where the orbital spin-moments cancel each other.

PACS numbers: 74.20.Pq, 71.15.Mb, 74.25.Ha, 74.25.Jb

## I. INTRODUCTION

Iron-based superconductors (FeSC) have attracted intense attention since the discovery of superconductivity in  $\text{LaFeAsO}_{1-x}\text{F}_x$  with  $T_C$  of 26 K.<sup>1</sup> A central topic of the studies is to understand the mechanism behind superconductivity. Since the electron-phonon coupling strength was proved to be insufficient to explain the relative high  $T_C$  both theoretically and experimentally,<sup>2-4</sup> spin fluctuations are expected as an alternative candidate for the pairing glue. Therefore understanding the magnetic behavior of the parent compounds is urgently needed.

Unexpectedly, the parent compounds of FeSC exhibit a wide variety of magnetic properties despite their similar crystal structures. The undoped compounds are antiferromagnetic metals with the moments ordered in stripes, i.e. ferromagnetically between the nearest Fe neighbors in one direction (x) and antiferromagnetically in the other (y). The moment of the 1111 compounds  $\text{RFeAsO}$  (R=rare earth) is  $\sim 0.3-0.8 \mu_B$ .<sup>5-8</sup> In the 122 compounds  $\text{AFe}_2\text{As}_2$  (A=Ca, Sr, Ba, Eu) it is  $\sim 0.8-1.0 \mu_B$ ,<sup>9-11</sup> whereas in the 111 family the moment is only  $\sim 0.09 \mu_B$  in  $\text{NaFeAs}$ <sup>12</sup> and could not be observed in  $\text{LiFeAs}$ .<sup>13</sup> In the 11 family, no local moment is found in  $\text{FeSe}$ ,<sup>14</sup> while  $\text{FeTe}$  has a unique magnetic structure, a so called double-stripe order, with a fairly big moment  $\sim 2.0 \mu_B$ .<sup>15</sup> This spread in magnetic moments is difficult to understand since the parent compounds have very similar lattice structures; they all have similar  $\text{FeX}$  (X=As, Se, Te) layers, and density functional theory (DFT) calculations give quite similar paramagnetic band structures for all the materials.<sup>16</sup>

It is conceivable that theoretical studies may clarify this puzzle. DFT with the local spin density approximation (LSDA) or the generalized gradient approximation (GGA) successfully reproduced the single-stripe antiferromagnetic (AFM) order in 1111 and 122 materials.<sup>17-20</sup> However the calculated magnetic moment is about  $1.5-2 \mu_B$ , which is much larger than the measured magnetic moment. Many theories have been proposed to explain

the outstanding discrepancy between DFT and experiment. Yildirim applied a fixed-spin-moment calculation to  $\text{LaFeAsO}$  and found the ground state with a moment of  $m = 0.48 \mu_B$ .<sup>21</sup> Nakamura *et al.* applied the LSDA+ $U$  approach to  $\text{LaFeAsO}_{1-x}\text{F}_x$  and reproduced the experimental moment with a *negative*  $U$ .<sup>22</sup> Mazin and Johannes argued that the small moment is due to the presence of antiphase boundaries.<sup>23</sup> Bascones *et al.* presented a five-band model and found a low moment state characterized by anti-parallel orbital magnetic moments.<sup>24</sup> However, it is still not clear which picture is more realistic.

In this work, we present an LSDA+ $U$  study to explain the puzzle of magnetism in FeSC. We show that the measured small magnetic moment can be reproduced with *positive*  $U$ , and its origin is a Coulomb-enhanced orbital hybridization between antiferromagnetic neighbors. Since the iron compounds are weak to moderately correlated systems,<sup>25,26</sup> the around-mean-field (AMF) functional<sup>27</sup> is employed in this work. All the calculations are performed with the full-potential linear augmented plane wave (FLAPW) within the local-density approximation, as implemented in package WIEN2K.<sup>28</sup> We concentrate on the 1111 material  $\text{LaFeAsO}$  and use the experimental lattice structure<sup>1</sup> with the space group  $\text{P4/nmm}$ ,  $a=4.035 \text{ \AA}$ ,  $c=8.7409 \text{ \AA}$ ,  $z_{\text{La}}=0.1415$  and  $z_{\text{As}}=0.6415$ . To study the single-stripe AFM order, we use the  $\sqrt{2} \times \sqrt{2} \times 1$  supercell containing 4 iron atoms. 144 k points are used within irreducible Brillouin zone. The muffin-tin sphere radii of 2.24, 2.28, 2.02 and 1.98  $a_0$  are used for La, Fe, As and O, respectively.

## II. RESULTS AND DISCUSSION

### A. Magnetism and band structure

Since LSDA+ $U$  may give multiple minima,<sup>29</sup> we change the starting magnetic moment on Fe to search for all the solutions. Fig. 1 shows our calculated local magnetic moment on Fe and the total energy as a func-

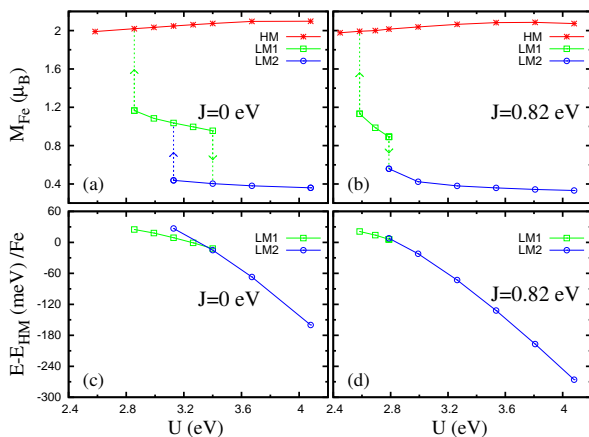


FIG. 1: Calculated magnetic moment and total energy for LaFeAsO as a function of  $U$ .

tion of the Coulomb interaction  $U$ . We used two values for the Hund's coupling,  $J=0$  and  $J=0.82$  eV, the latter having been obtained from an X-ray experiment.<sup>26</sup> Surprisingly, two kinds of low moment (LM) in addition to one high moment (HM) solutions are found in our calculations. The HM state was expected since the LSDA+ $U$  is usually believed to have a tendency to enhance the magnetic moment. The two LM states have the magnetic moments  $m \sim 1.0 \mu_B$  (LM1) and  $m \sim 0.4 \mu_B$  (LM2), which are in good agreement with the measured moments in the 122 compounds and in most of the 1111 compounds, respectively. We did the same calculation for the 122 materials  $\text{BaFe}_2\text{As}_2$ , and also found two LM states, very similar to LaFeAsO.

As shown in Fig. 1a and 1b, the LM1 state only exists within a certain  $U$  range, and it can jump to the HM or LM2 states with a discontinuous change of the magnetic moment when  $U$  decreases or increases. The LM2 state requires larger  $U$  and shows slight variation in moment when  $U$  is increasing. Fig. 1c and 1d present the total energy of the LM1 and LM2 states relative to the HM state. The figure shows that a small  $U$  favors the HM state and a large  $U$  favors the LM2 state. Consequently, the experimental ground state of LaFeAsO<sup>5</sup> can be reproduced in our calculation if  $U$  is large enough. The effect of  $J$  may also be seen in Fig. 1. In general, the results for  $J=0$  and  $J=0.82$  eV are similar. We therefore only consider the case of  $J=0$  in the following parts of this work.

Our theoretical band structures of LaFeAsO for the different states are presented in Fig. 2. The LM1 and LM2 states show very different band structures. The LM1 indicates a rather good metal while the LM2 state is nearly semiconducting. Therefore, the magnetic strength and electrical conductivity are correlated properties in the iron compounds. The coexistence of the LM1 and LM2 states in our calculations may clarify some seemingly inconsistent experiments. McGuire *et al.*<sup>30</sup> reported a systematic study on the 1111 materials. They found that

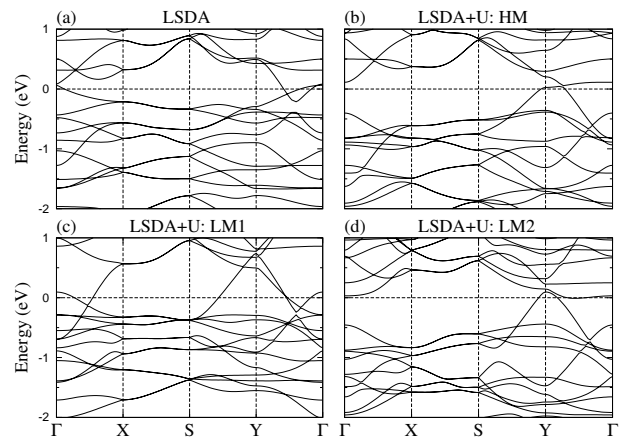


FIG. 2: Theoretical band structures of LaFeAsO for single-stripe AFM state. All the LSDA+ $U$  band structures are for  $J=0$  and  $U=3.26$  eV.

CeFeAsO has a magnetic moment about  $0.3 \mu_B$  and its low temperatures electrical resistivity is  $\rho_0=2$  m $\Omega$  cm. While neutron scattering experiment by Zhao *et al.*<sup>6</sup> indicated a magnetic moment of  $0.8 \mu_B$  for CeFeAsO, and Jesche *et al.*<sup>31</sup> reported an electrical resistivity of  $\rho_0=140 \mu\Omega$  cm for CeFeAsO. It should be noticed that McGuire *et al.* used polycrystalline samples and Jesche *et al.* used large single crystals. Moreover, a recent neutron scattering experiment<sup>32</sup> found single crystal LaFeAsO has a moment of  $0.8 \mu_B$ , which is also very different from the earlier study.<sup>5</sup> From our theory, these discrepancies can be naturally explained by assuming that the samples were in different states, which may be due to the quality of samples.

## B. Origin of the low moment states

In the LSDA+ $U$  calculations, the on-site elements of the density matrix may contain some important information about the detail of the states. In Table I, we present the occupancy of the Fe 3d orbitals and the contribution of each orbital to the spin magnetic moment. The main elements of the spin-dependent local density matrices can be extracted from this table. The main difference between the three LSDA+ $U$  states lies in the moment of the  $xy$  orbital. In the HM state,  $m_{xy}$  is enhanced from the LSDA value of  $0.42 \mu_B$  to  $0.52 \mu_B$ . But in the LM1 and LM2 states,  $m_{xy}$  is reduced to 0 and  $-0.43 \mu_B$ ! This unusual reduction implies that the  $xy$  orbital is the key to understand the LM states. The HM, LM1 and LM2 states may be characterized as  $m_{xy} > 0$ ,  $m_{xy} \sim 0$  and  $m_{xy} < 0$ , respectively. We may therefore name the LM states as 'orbital-spin ordered' states. In the LM2 state,  $m_{xy}$  and  $m_{yz}$  have opposite signs from  $m_{x^2-y^2}$  and  $m_{xz}$ . It is worth noting that this result is in very good agreement with the tight-binding study<sup>24</sup> by Bascones *et al.*

Compared with the LSDA solution, LSDA+ $U$  rear-

TABLE I: Occupancy of the Fe 3d orbitals and orbital contribution to spin magnetic moment. The data for different solutions correspond to the band structures in Fig. 2. All the LSDA+ $U$  data are obtained with  $J=0$  and  $U=3.26$  eV.

	$3z^2 - r^2$	$x^2 - y^2$	$xy$	$xz$	$yz$	total
LSDA						
occupancy	1.29	1.19	1.21	1.15	1.34	6.19
moment	0.35	0.30	0.42	0.44	0.25	1.76
LSDA+ $U$ : HM						
occupancy	1.25	1.16	1.19	1.09	1.47	6.16
moment	0.43	0.42	0.52	0.56	0.13	2.05
LSDA+ $U$ : LM1						
occupancy	1.37	0.98	1.45	1.06	1.33	6.19
moment	0.06	0.28	0.00	0.57	0.08	0.99
LSDA+ $U$ : LM2						
occupancy	1.36	1.05	1.24	1.08	1.44	6.18
moment	0.03	0.31	-0.43	0.55	-0.05	0.41

ranges the orbital occupancy and orbital spin-moment. The LSDA+ $U$  method can be mapped onto a single-band picture if there is no strong orbital hybridization. In this case, the Coulomb interaction has two possible effects on the magnetic moment. The first is to enhance the exchange splitting between the majority spin and minority spin, which causes larger moment for each orbital. The second is to induce a charge transfer from the less occupied orbitals to more occupied orbitals, which may decrease the moment of the most occupied orbital. As may be seen, the HM solution agrees well with this picture, but the strong rearrangement of  $m_{xy}$  and  $m_{3z^2-r^2}$  in the LM solutions cannot be understood. The deficiency of the single-band picture suggests that interorbital coupling plays an important role in the LM states. This has been realized by Bascones *et al.*<sup>24</sup> They stressed that it is important to include all five  $d$  orbitals in model studies.

Fig. 3 shows the band character for the  $d_{3z^2-r^2}^\sigma$  and  $d_{xy}^{\bar{\sigma}}$  orbitals, where  $\sigma$  stands for the majority spin and  $\bar{\sigma}$  for the minority spin. One may see that the hybridization of these two orbitals is strongly enhanced in the LM states relative to the LSDA solution. This strong hybridization between different spin channels (or more precisely, between antiferromagnetic neighbors) rationalizes the reduction of  $m_{xy}$  and  $m_{3z^2-r^2}$  in the LM states. Similar enhanced hybridization is also found between some other antiferromagnetic orbitals, such as  $d_{x^2-y^2}^\sigma - d_{xy}^{\bar{\sigma}}$  and  $d_{yz}^\sigma - d_{xy}^{\bar{\sigma}}$ . Here we focus on this  $d_{3z^2-r^2}^\sigma - d_{xy}^{\bar{\sigma}}$  hybridization. The strength of orbital hybridization depends on two factors: hopping integral and orbital on-site energy. In the LSDA+ $U$  approach,  $U$  does not change the hopping integrals, but shifts the on-site energies. As shown in Fig. 3, the  $d_{3z^2-r^2}^\sigma$  and  $d_{xy}^{\bar{\sigma}}$  bands are much closer in the LM solutions than those in the LSDA solution, which is responsible for the enhancement of orbital hybridization.

In a tight-binding model, the  $d$  orbital on-site energy

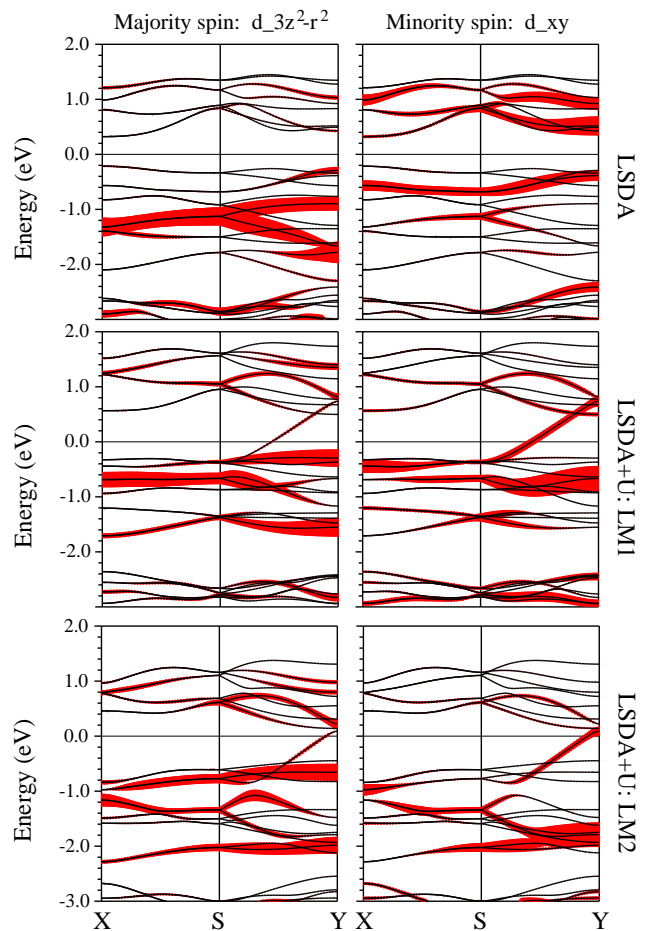


FIG. 3: Band character for the LSDA, LM1 and LM2 solutions. The left panels are for the  $3z^2 - r^2$  orbital with majority spin, the right panels for the  $xy$  orbital with minority spin.

can be written as

$$\epsilon_\alpha^\sigma = \epsilon_\alpha^0 \pm \frac{1}{2}Im - Un_\alpha^\sigma + \epsilon_{dc}^\sigma. \quad (1)$$

where  $\epsilon$  stands for the on-site energy,  $\alpha$  for the orbital,  $\sigma$  for the spin,  $m$  for the local magnetic moment,  $n$  for the occupancy number.  $I$  is the Stoner exchange integral, which is about 0.9 eV in metallic Fe.<sup>33</sup> The minus (plus) sign of the term  $\frac{1}{2}Im$  is for the spin that is parallel (anti-parallel) to the direction of the local magnetic moment.  $\epsilon_{dc}^\sigma$  corresponds to the double counting term of the LSDA+ $U$  method. In this work, we use the AMF functional<sup>27</sup> and have  $\epsilon_{dc}^\sigma = U \sum_\alpha n_\alpha^\sigma / 5$  for the  $d$  orbitals. For two orbitals with opposite spins, we get

$$(\epsilon_\alpha^\sigma - \epsilon_\beta^{\bar{\sigma}}) = -Im - U(n_\alpha^\sigma - n_\beta^{\bar{\sigma}}) + (\epsilon_{dc}^\sigma - \epsilon_{dc}^{\bar{\sigma}}) + (\epsilon_\alpha^0 - \epsilon_\beta^0). \quad (2)$$

It is reasonable to assume  $(\epsilon_{3z^2-r^2}^0 - \epsilon_{xy}^0) = 0$ , as the LSDA solution shows that the  $3z^2 - r^2$  and  $xy$  orbitals have similar occupancies. Then we can calculate the gap between the  $d_{3z^2-r^2}^\sigma$  and  $d_{xy}^{\bar{\sigma}}$  orbitals. Using the data in Table I, we get -1.58 eV for the LSDA, -0.22 eV for the LM1 and 0.35 eV for the LM2. These values are

consistent with the character bands shown in Fig. 3. To enhance the hybridization, the  $d_{3z^2-r^2}^\sigma$  and  $d_{xy}^\sigma$  orbitals need to be close. Eq. 2 shows some competitive factors for this requirement. The term  $-Im$  opens a gap between opposite spins, and therefore the  $U$  term and the double counting term need to offset this splitting. This gives a restriction on  $U$ . As shown in Fig. 1, there is no LM solution when  $U$  is too small. For the LSDA state, the exchange splitting  $-Im$  opens a gap of  $-1.58$  eV. If we start the LSDA+ $U$  calculation with the LSDA solution, this gap is too large to be overcome and the system is easier to converge to the HM state. To search for the LM solutions, we need to start the LSDA+ $U$  calculation with a small magnetic moment. This may be the technical reason why the LM states were not found before.

We have shown that the role of  $U$  in the LM states is to enhance the orbital hybridization between antiferromagnetic neighbors by changing the on-site energies. Here we discuss the effect of  $d$ - $d$  interorbital hopping, which is the other factor influencing the strength of hybridization. From the structure of LaFeAsO, we may realize that the direct interaction between the  $d_{xy}$  and  $d_{3z^2-r^2}$  orbitals is weak, and therefore the hybridization of  $d_{3z^2-r^2}^\sigma$  and  $d_{xy}^\sigma$  is via the As  $p$  orbitals. These  $p$ - $d$  interactions, such as  $p_z$ - $d_{xy}$  and  $p_z$ - $d_{3z^2-r^2}$ , are very sensitive to the Fe-As-Fe angle. This characteristic can be used to tune the  $d$ - $d$  interorbital hoppings. We adjust the Fe-As-Fe angle by changing the ratio between lattice constant  $c$  and  $a$  while keeping the volume constant. Our calculated magnetic moment of LaFeAsO as a function of  $c/a$  is shown in Fig. 4. The  $x$ -axis of the figure is labelled  $z_{As}/a$ , where  $z_{As}$  is the height of the As atom above the nearest Fe layer. In the LM2 state,  $m_{xy}$  is anti-parallel to the direction of the total moment at small  $z_{As}/a$  as shown in Table I. As  $z_{As}/a$  increases,  $m_{xy}$  becomes numerically larger and eventually the total moment gets the same direction as  $m_{xy}$ , which is indicated by the negative sign in Fig. 4. The figure shows that the LSDA state has a very weak dependence on the value of  $z_{As}/a$ . Please note that the Fe-As distance almost keeps a constant in this calculation. On the other hand, the LM states show very strong dependence on the FeAs<sub>4</sub> geometry. This phenomenon confirms the importance of the interorbital coupling to the LM states. We may conclude that the origin of the LM solutions is the Coulomb-enhanced orbital hybridization between antiferromagnetic neighbors.

### C. Low moment solution from GGA

Fig. 1 indicates a critical value  $U_c$  for the LSDA+ $U$  calculations: the LM states only exist at  $U > U_c$ . According to our explanation for the LM states, the Coulomb interaction and FeAs<sub>4</sub> structure are the two factors giving rise to the orbital-spin ordered states. Then  $U_c$  may be reduced by changing the FeAs<sub>4</sub> geometry. We find that  $U_c$  for NaFeAs is about 1.9 eV, which is much

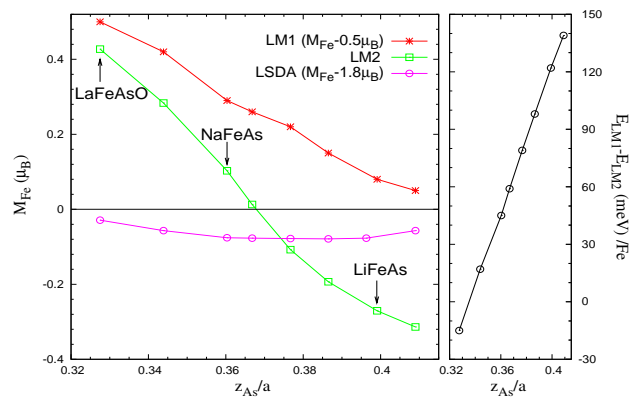


FIG. 4: Magnetic moment and total energy of LaFeAsO as a function of  $c/a$  with constant volume. The magnetic moment for LM1 and LSDA are shifted to fit the window. The experimental values of  $z_{As}/a$  for LaFeAsO, NaFeAs and LiFeAs are indicated by arrows. The LSDA+ $U$  data are calculated with  $J=0$  and  $U=3.26$  eV.

smaller than the value for LaFeAsO ( $\sim 2.8$  eV). An interesting question is raised: can LSDA or GGA produce the LM states without  $U$ ?

Fig. 5 shows the low moment solution we find with GGA (without  $U$ ). The GGA-LM state appears at  $z_{As}/a=0.40$ , and the total magnetic moment reaches a maximum at  $z_{As}/a=0.46$ . The GGA-LM solution is not a simple low moment state, but an orbital-spin ordered state. At  $z_{As}/a=0.46$ , the orbital moments are  $m_{3z^2-r^2}=0.02$ ,  $m_{x^2-y^2}=0.04$ ,  $m_{xy}=-0.23$ ,  $m_{xz}=0.33$  and  $m_{yz}=0.01 \mu_B$ . We also present the band structure for  $z_{As}/a=0.46$  in Fig. 5. The very different band dispersion along  $x$  direction and  $y$  direction shows that this state is far away from the paramagnetic phase although it has a small total moment. As may be seen, the GGA-LM band structure is a little bit similar to the LM2 band structure shown in Fig. 2, while the main difference is the Coulomb interaction nearly opens a gap at Fermi level. Interestingly, we find that LSDA can hardly produce this low moment state. A possible reason is that LSDA contains less electron correlation in the iron compounds than GGA does.

The LSDA+ $U$  method is sometimes questioned due to the double counting problem.<sup>29,34</sup> The choice of LSDA+ $U$  functional is somewhat arbitrary. The GGA-LM state proves that the orbital-spin ordering does not come from a specific LSDA+ $U$  functional, but originates in the tetrahedral structure of FeAs<sub>4</sub>. The GGA-LM state provides a strong evidence for the orbital-spin ordering in FeSC and also confirms our explanation for the LM states.

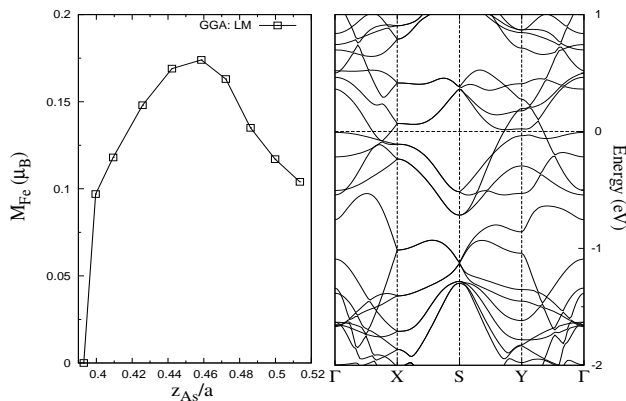


FIG. 5: Low moment state in LaFeAsO calculated by GGA (WITHOUT  $U$ ). The left panel is the magnetic moment as a function of  $c/a$  with constant volume. The right panel is the band structure for  $z_{As}/a = 0.46$ , which is corresponding to an orbital-spin ordered state with  $m_{tot} = 0.17$ ,  $m_{xy} = -0.23$  and  $m_{xz} = 0.33 \mu_B$ .

#### D. FeAs<sub>4</sub> geometry, magnetism and high-pressure experiments

It is known that the FeAs<sub>4</sub> tetrahedron tends to have similar volume in different iron-arsenides, while its geometry is tuned by different inserted layers (see Table I of Ref. 16). For example, LiFeAs has the largest As height  $z_{As}$  in all iron-arsenides while its lattice constant  $a$  is the smallest. Therefore, Fig. 4 allows us to estimate the magnetic moments of the 111 materials. The figure gives a moment of  $0.1 \mu_B$  for NaFeAs and  $-0.27 \mu_B$  for LiFeAs. Here we consider the LM2 state because the LM2 state becomes more and more energetically favorable when  $z_{As}/a$  is increasing as shown in Fig. 4. To check these estimated values, we did a direct calculation using the experimental structures, which gives  $m=0.04 \mu_B$  for NaFeAs and  $m=-0.20 \mu_B$  for LiFeAs. This agreement between the estimation and calculation shows that the FeAs<sub>4</sub> geometry is a very important factor controlling the magnetic properties of FeSC, which is responsible for the variety of magnetic moments in the 1111 and 111 materials. Our calculated magnetic moment for NaFeAs,  $m=0.04 \mu_B$ , is in good agreement with the measured value.<sup>12</sup> But in contrast to the experiment,<sup>13</sup> the ground state of LiFeAs in our calculation has the single-stripe AFM order. Actually, there might be experimental evidence for the striped AFM order. Borisenko *et al.* measured the Fermi surface of LiFeAs using angle-resolved photoemission.<sup>35</sup> They found that the pocket around the  $\Gamma$  point is shaped like a butterfly, which indicates that the 4-fold rotation symmetry is broken. This symmetry breaking might be due to the striped AFM order.

Fig. 4 may also explain the behavior of the parent compounds under pressure. High-pressure experiment shows that the undoped LaFeAsO becomes superconducting at pressure  $\sim 2$  GPa and reaches a maximum  $T_C$  of 21 K

at  $\sim 12$  GPa. For higher pressures the  $T_C$  decreases slowly.<sup>36</sup> LiFeAs shows very different pressure behavior from LaFeAsO. LiFeAs is a superconductor without external pressure. Under pressure, the  $T_C$  of LiFeAs decreases linearly at a rate of 1.5 K/GPa,<sup>37</sup> which means that the maximal  $T_C$  is at zero pressure. Interestingly, a different high-pressure experiment indicated that the behavior of NaFeAs is more similar to LaFeAsO than LiFeAs,<sup>38</sup> even though NaFeAs and LiFeAs belong to the same family.

To explain these experiments, we need to consider the structural distortion under pressure. Pressure experiments have shown that the Fe-As bond length is very rigid while the Fe-Fe distance shrinks much faster when pressure increases,<sup>39,40</sup> i.e.,  $z_{As}/a$  increased by pressure. It is found that chemical doping and pressure can both induce superconductivity in BaFe<sub>2</sub>As<sub>2</sub> and they have very similar influence on the FeAs<sub>4</sub> geometry.<sup>39,41</sup> A noticeable fact is that chemical doping hardly changes the crystal volume.<sup>41</sup> This finding shows that the FeAs<sub>4</sub> geometry is the key structural feature to superconductivity,<sup>39</sup> whereas the volume reduction under pressure is less important. Therefore the  $x$ -axis direction of Fig. 4 can be regarded as the direction of increasing pressure.

We consider the LM2 state in Fig. 4. For LaFeAsO and NaFeAs, pressure first suppresses the magnetism. After the magnetic moment reaches 0, the pressure starts to enhance the magnetism. It is known that the emergence of superconductivity in the FeSC is related to the suppression of magnetism. Then the decreasing magnetism corresponds to the increasing  $T_C$ , conversely, the increasing magnetism corresponds to the decreasing  $T_C$ . And the maximal  $T_C$  occurs at the magnetic moment  $m=0$ . For LiFeAs, pressure can only enhance the magnetism as shown in Fig. 4. Consequently, the  $T_C$  of LiFeAs has a negative pressure coefficient,  $dT_C/dP < 0$ . Therefore, these different high-pressure experiments can be consistently explained by our theory. Fig. 4 shows that the LM2 state is more and more energetically favorable than the LM1 state when  $z_{As}/a$  increases; hence the 122 compounds, which have the LM1 ground state at 0 pressure, will enter into the LM2 state when pressure increases. Then our explanation for the high-pressure experiments is also suitable for the 122 materials. Importantly, in this picture, the suppression of magnetism is because the orbital spin-moments cancel each other. This suggests the superconducting phase is not a 'real' nonmagnetic state but an orbital-spin ordered state.

#### E. LSDA+ $U$ functionals

In this work, we used the AMF LSDA+ $U$  functional. We also checked our calculation with another widely used scheme: the fully localized limit (FLL) functional,<sup>42</sup> which is suggested to be more suitable for strongly correlated systems. We found one LM solution coexists with a HM solution in this functional. The LM solution is very

similar to the LM2 state and shows very similar  $z_{As}/a$  dependence. However, we didn't find the LM1 solution, and FLL energetically favors the HM solution.

### III. SUMMARY

In summary, we have studied the magnetic properties of iron-arsenides using the LSDA+ $U$  approach. Two low moment states are found in our calculation, which reproduce the measured magnetic moments in the 1111 and 122 materials well. The LM2 state shows good agreement with the low moment state found by previous tight-binding study. Our study reveals that the origin of the low magnetization is the strong orbital hybridization between antiferromagnetic neighbors. From the picture in-

dicated above we have learned: Firstly, the geometry of FeAs<sub>4</sub> is crucial to superconductivity and magnetism because it controls the  $d$ - $d$  interorbital coupling. Secondly, our theory suggests that the superconducting phase is not a conventional nonmagnetic state, but a state where the orbital spin-moments cancel each other. This implies an inherent relationship between the magnetic correlation and superconductivity.

### Acknowledgments

The author gratefully acknowledges O. K. Andersen, O. Jepsen, L. Boeri and A. N. Yaresko for helpful discussions and useful comments.

- 
- <sup>1</sup> Y. Kamihara, T. Watanabe, M. Hirano, and H. Hosono, *J. Am. Chem. Soc.* **130**, 3296 (2008).
- <sup>2</sup> L. Boeri, O. V. Dolgov, and A. A. Golubov, *Phys. Rev. Lett.* **101**, 026403 (2008).
- <sup>3</sup> L. Boeri, M. Calandra, I. I. Mazin, O. V. Dolgov, and F. Mauri *Phys. Rev. B* **82**, 020506(R) (2010).
- <sup>4</sup> A. D. Christianson, M. D. Lumsden, O. Delaire, M. B. Stone, D. L. Abernathy, M. A. McGuire, A. S. Sefat, R. Jin, B. C. Sales, D. Mandrus, E. D. Mun, P. C. Canfield, J. Y. Y. Lin, M. Lucas, M. Kresch, J. B. Keith, B. Fultz, E. A. Goremychkin, and R. J. McQueeney, *Phys. Rev. Lett.* **101**, 157004 (2008).
- <sup>5</sup> Clarina de la Cruz, Q. Huang, J. W. Lynn, Jiying Li, W. Ratcliff, J. L. Zarestky, H. A. Mook, G. F. Chen, J. L. Luo, N. L. Wang and Pengcheng Dai, *Nature* **453**, 899-902 (2008).
- <sup>6</sup> J. Zhao, Q. Huang, C. de la Cruz, S. Li, J. W. Lynn, Y. Chen, M. A. Green, G. F. Chen, G. Li, Z. Li, J. L. Luo, N. L. Wang, and P. Dai, *Nat. Mater.* **7**, 953 (2008).
- <sup>7</sup> S. A. J. Kimber, D. N. Argyriou, F. Yokaichiya, K. Habicht, S. Gerischer, T. Hansen, T. Chatterji, R. Klingeler, C. Hess, G. Behr, A. Kondrat, and B. Buchner, *Phys. Rev. B* **78**, 140503 (2008).
- <sup>8</sup> Y. Qiu, Wei Bao, Q. Huang, T. Yildirim, J. M. Simmons, M. A. Green, J. W. Lynn, Y. C. Gasparovic, J. Li, T. Wu, G. Wu, and X. H. Chen, *Phys. Rev. Lett.* **101**, 257002 (2008).
- <sup>9</sup> A. I. Goldman, D. N. Argyriou, B. Ouladdiaf, T. Chatterji, A. Kreyssig, S. Nandi, N. Ni, S. L. Budko, P. C. Canfield, and R. J. McQueeney, *Phys. Rev. B* **78**, 100506(R) (2008)
- <sup>10</sup> Jun Zhao, W. Ratcliff, J. W. Lynn, G. F. Chen, J. L. Luo, N. L. Wang, Jiangping Hu, and Pengcheng Dai, *Phys. Rev. B* **78**, 140504(R) (2008).
- <sup>11</sup> Y. Su, P. Link, A. Schneidewind, Th. Wolf, P. Adelman, Y. Xiao, M. Meven, R. Mittal, M. Rotter, D. Johrendt, Th. Brueckel, and M. Loewenhaupt, *Phys. Rev. B* **79**, 064504 (2009).
- <sup>12</sup> Shiliang Li, Clarina de la Cruz, Q. Huang, G. F. Chen, T.-L. Xia, J. L. Luo, N. L. Wang, and Pengcheng Dai, *Phys. Rev. B* **80**, 020504(R) (2009).
- <sup>13</sup> Joshua H. Tapp, Zhongjia Tang, Bing Lv, Kalyan Sasmal, Bernd Lorenz, Paul C. W. Chu, and Arnold M. Guloy, *Phys. Rev. B* **78**, 060505(R) (2008).
- <sup>14</sup> S. Medvedev, T. M. McQueen, I. A. Troyan, T. Palasyuk, M. I. Erements, R. J. Cava, S. Naghavi, F. Casper, V. Ksenofontov, G. Wortmann and C. Felser, *Nat. Mater.* **8**, 630-633 (2009).
- <sup>15</sup> Shiliang Li, Clarina de la Cruz, Q. Huang, Y. Chen, J. W. Lynn, Jiangping Hu, Yi-Lin Huang, Fong-Chi Hsu, Kuo-Wei Yeh, Maw-Kuen Wu, and Pengcheng Dai, *Phys. Rev. B* **79**, 054503 (2009).
- <sup>16</sup> T. Miyake, K. Nakamura, R. Arita and M. Imada, *J. Phys. Soc. Jpn.* **79**, 044705 (2010).
- <sup>17</sup> S. Ishibashi, K. Terakura, and H. Hosono, *J. Phys. Soc. Jpn.* **77**, 053709 (2008).
- <sup>18</sup> Z. P. Yin, S. Lebegue, M. J. Han, B. P. Neal, S. Y. Savrasov, and W. E. Pickett, *Phys. Rev. Lett.* **101**, 047001 (2008).
- <sup>19</sup> D.J. Singh, *Phys. Rev. B* **78**, 094511 (2008).
- <sup>20</sup> A. N. Yaresko, G.-Q. Liu, V. N. Antonov, and O. K. Andersen, *Phys. Rev. B* **79**, 144421 (2009).
- <sup>21</sup> T. Yildirim, *Phys. Rev. Lett.* **101**, 057010 (2008).
- <sup>22</sup> H. Nakamura, N. Hayashi, N. Nakai, and M. Machida, *J. Phys. Soc. Jpn.* **77**, Suppl. C, 153 (2008).
- <sup>23</sup> I.I. Mazin and M. D. Johannes, *Nature Phys.* **5**, 141 (2009).
- <sup>24</sup> E. Bascones, M. J. Calderon, and B. Valenzuela, *Phys. Rev. Lett.* **104**, 227201 (2010).
- <sup>25</sup> K. Nakamura, R. Arita, and M. Imada, *J. Phys. Soc. Jpn.* **77**, 093711 (2008).
- <sup>26</sup> W. L. Yang, A. P. Sorini, C.-C. Chen, B. Moritz, W.-S. Lee, F. Vernay, P. Olalde-Velasco, J. D. Denlinger, B. Delley, J.-H. Chu, J. G. Analytis, I. R. Fisher, Z. A. Ren, J. Yang, W. Lu, Z. X. Zhao, J. van den Brink, Z. Hussain, Z.-X. Shen, and T. P. Devereaux, *Phys. Rev. B* **80**, 014508 (2009).
- <sup>27</sup> M. T. Czyzyk and G. A. Sawatzky, *Phys. Rev. B* **49**, 14211 (1994).
- <sup>28</sup> P. Blaha, K. Schwarz, G. Madsen, D. Kvasnicka and J. Luitz, Computer code WIEN2K, TU Wien, Vienna, 2001.
- <sup>29</sup> E. R. Ylvisaker, W. E. Pickett, and K. Koepfner, *Phys. Rev. B* **79**, 035103 (2009).
- <sup>30</sup> M. A. McGuire, R. P. Hermann, A. S. Sefat, B. C. Sales, R. Jin, D. Mandrus, F. Grandjean and G. J. Long, *New Journal Physics* **11**, 025011 (2009).
- <sup>31</sup> A. Jesche, C. Krellner, M. de Souza, M. Lang, and C.



- Geibel, Phys. Rev. B **81**, 134525 (2010).
- <sup>32</sup> H.-F. Li, W. Tian, J.-Q. Yan, J. L. Zarestky, R. W. McCallum, T. A. Lograsso, and D. Vaknin, Phys. Rev. B **82**, 064409 (2010).
- <sup>33</sup> O.K. Andersen, J. Madsen, U.K. Poulsen, O. Jepsen and J. Kollar, Physica B **86-88** (1977) 249.
- <sup>34</sup> A. G. Petukhov, I. I. Mazin, L. Chioncel, and A. I. Lichtenstein, Phys. Rev. B **67**, 153106 (2003).
- <sup>35</sup> S. V. Borisenko, V. B. Zabolotnyy, D. V. Evtushinsky, T. K. Kim, I. V. Morozov, A. N. Yaresko, A. A. Kordyuk, G. Behr, A. Vasiliev, R. Follath, and B. Buchner, Phys. Rev. Lett. **105**, 067002 (2010).
- <sup>36</sup> H. Okada, K. Igawa, H. Takahashi, Y. Kamihara, M. Hirano, H. Hosono, K. Matsubayashi, and Y. Uwatoko, J. Phys. Soc. Jpn. **77**, 113712 (2008).
- <sup>37</sup> M. Gooch, B. Lv, J. H. Tapp, Z. Tang, B. Lorenz, A. M. Guloy and P. C. W. Chu, EPL **85**, 27005 (2009).
- <sup>38</sup> S. J. Zhang, X. C. Wang, Q. Q. Liu, Y. X. Lv, X. H. Yu, Z. J. Lin, Y. S. Zhao, L. Wang, Y. Ding, H. K. Mao and C. Q. Jin, EPL **88**, 47008 (2009).
- <sup>39</sup> S. A. J. Kimber, A. Kreyssig, Y.-Z. Zhang, H. O. Jeschke, R. Valenti, F. Yokaichiya, E. Colombier, J. Yan, T. C. Hansen, T. Chatterji, R. J. McQueeney, P. C. Canfield, A. I. Goldman and D. N. Argyriou, Nature Mater. **8**, 471-475 (2009).
- <sup>40</sup> M. Mito, M. J. Pitcher, W. Crichton, G. Garbarino, P. J. Baker, S. J. Blundell, P. Adamson, D. R. Parker and S. J. Clarke, J. Am. Chem. Soc. **131**, 2986-1992 (2009).
- <sup>41</sup> M. Rotter, M. Pangerl, M. Tegel, and D. Johrendt, Angew. chem. **47** 7949 (2008).
- <sup>42</sup> V. I. Anisimov, I. V. Solovyev, M. A. Korotin, M. T. Czyzyk and G. A. Sawatzky, Phys. Rev. B **48**, 16929 (1993).